

Article

Large-Scale Hydrological Modeling and Decision-Making for Agricultural Water Consumption and Allocation in the Main Stem Tarim River, China

Yang Yu ^{1,2,*}, Markus Disse ¹, Ruide Yu ², Guoan Yu ^{1,3}, Lingxiao Sun ², Philipp Huttner ¹ and Christian Rumbaur ¹

¹ Chair of Hydrology and River Basin Management, Technical University of Munich (TUM), Arcisstrasse 21, Munich 80333, Germany; E-Mails: markus.disse@tum.de (M.D.); yuga@igsnr.ac.cn (G.Y.); philipp.huttner@mytum.de (P.H.); christian.rumbaur@tum.de (C.R.)

² Xinjiang Institute of Ecology and Geography, Chinese Academy of Sciences (CAS), No. 818 South Beijing Road, Urumqi 830011, Xinjiang, China; E-Mails: yuruide@sina.com (R.Y.); xjlyxx@163.com (L.S.)

³ Key Laboratory of Water Cycle and Related Land Surface Processes, Institute of Geographic Sciences and Natural Resources Research, Chinese Academy of Sciences, 11A Datun Road, Chaoyang District, Beijing 100101, China

* Author to whom correspondence should be addressed; E-Mail: yang.yu@tum.de or yysnowcs@163.com; Tel.: +49-89-289-23229; Fax: +49-89-289-23221.

Academic Editor: Athanasios Loukas

Received: 2 April 2015 / Accepted: 3 June 2015 / Published: 12 June 2015

Abstract: A large-scale hydrological model (MIKE HYDRO) was established for the purpose of sustainable agricultural water management in the main stem Tarim River, located in northwest China. In this arid region, agricultural water consumption and allocation management are crucial to address the conflicts among irrigation water users from upstream to downstream. The results of model calibration indicated a close correlation between simulated and observed values. Scenarios with the change on irrigation strategies and land use distributions were investigated. Irrigation scenarios revealed that the available irrigation water has significant and varying effects on the yields of different crops. Irrigation water saving could reach up to 40% in the water-saving irrigation scenario. Land use scenarios illustrated that an increase of farmland area in the lower reach gravely aggravated the water deficit, while a decrease of farmland in the upper reaches resulted in considerable benefits for all sub-catchments. A substitution of crops was also investigated, which demonstrated

the potential for saving considerable amounts of irrigation water in upper and middle reaches. Overall, the results of this study provide a scientific basis for decision-making on agricultural water consumption and allocation in the study area.

Keywords: MIKE HYDRO; water scarcity; agricultural water allocation; irrigation water demand; irrigation and land use scenarios; Tarim River basin

1. Introduction

Water scarcity is expected to increase in the dry regions of Asia [1]. Increasing population and farming practices will increase the stress on water resources in these arid regions. The needs of natural ecosystems have become another source of competition that increases pressure on water resources in the future [2]. The management of irrigation water use continues to pose increasing challenges to decision-makers and planners in developing countries, particularly those facing limited water resources. The Tarim River is one of the largest inland rivers in the world and located in the northwest of China, known worldwide for its extreme climatic situation and vulnerable ecosystem. With the high-intensity and large-scale exploitation of water resources at the upper reaches of the Tarim River, the water curtailment downstream has brought great negative effects for the ecosystem in the Tarim River basin [3,4].

The Tarim River originates at the confluence of the Aksu, Yarkand, Hotan and Kaidu-Konqi rivers, and flows into the Taitema Lake, east of Xinjiang. With a main stem of 1321 km, it is the longest inland river in China. The total area of the Tarim River basin is 1.02×10^6 km². The basin contains 42 counties and cities, with a total population of 8.26×10^6 . The basin has become the most important source of cotton in China. Due to relatively low rainfall in the region, irrigation is the primary source of water for agriculture along the Tarim River [5]. Although the volume of flow from the river's headwaters is sensitive to precipitation [6], the main stem of the river is dominated by human activities such as agricultural irrigation [7]. Water allocations specify the amount of water that can be extracted each year by license holders. During the past six decades, as conflicts among the water users from upstream to downstream has continuously been severe, and intensive exploitation of water resources has caused serious environmental problems in the basin, a comprehensive spatial-temporal assessment of variability in flows and water allocation is imperative to work towards sustainable management of water resources on the Tarim River.

Previous studies show that, due to the effects of climate change, annual runoff in the river's headwaters has significantly increased since the 1950s. Average air temperature experienced a significant increase in the last few decades, and average annual precipitation increased by 6–8 mm per decade [6]. However, surface runoff in the main stem has dramatically decreased in the 1970s, 1980s and 1990s [7]. Since the 1970s, less than 1/4 of the discharge from the main stem of the Tarim River has been reaching the downstream areas in the average year. However, the lower reach of the river serves as the "Green Corridor" in protecting the natural environment from encroachment by the Taklamakan and Kuluk deserts. The Green Corridor is an essential ecological corridor for maintaining ecosystem balance in the lower reach. Its area has sharply reduced because of serious wind erosion, land desertification and

degeneration of natural vegetation [4]. This indicates the challenge of maintaining sustainable water resources in the river oases. In this extremely arid region close to Taklamakan Desert, water is the key factor in maintaining local ecosystems. Increased farming and water use since the 1950s have led to significant hydrological and environmental degradation [8–13]. In this context, water saving and higher crop irrigation efficiencies are crucial to the future allocation of water resources.

Large-scale hydrological models have been used to assess the impacts of land use changes and other human activities on water resources [14–16]. These models represent a compromise between the limited insight obtained from a lumped model and the large amount of data and computational power required from a distributed model. Consequently, a more suitable approach would be a semi-distributed model wherein the overland flow and unsaturated zone are represented by their lumped-parameter semi-empirical counterparts to simplify the overall analysis [17]. MIKE HYDRO is an integrated, multipurpose, map-based decision support tool developed by the Danish Hydraulic Institute (DHI). The Basin model type is the MIKE HYDRO module used for a variety of model applications, covering integrated water resources management (IWRM), water resources assessment, water allocation, reservoir operation and other types of analysis [18]. It enables detailed simulations of water resources and land use in the catchment areas. The scale of these models may range from large river basins to smaller local projects.

This study aims to simulate the possible effects of irrigation and land use scenarios in water savings for the main stem of the Tarim River. Higher crop irrigation efficiencies and optimized water allocation strategies are discussed to seek practical approach of increasing ecological water for the restoration of downstream Green Corridor. The study is an important part of the five-year SuMaRiO (Sustainable Management of River Oases along the Tarim River/China, 2011–2016) project. Section 2 describes the development of the large-scale hydrological model for the main stem of the Tarim River, including routing method, definition of the four sub-catchments, crop modules and the calibration of monthly data from three gauging stations. Section 3 describes the design of scenarios for irrigation and land use at the sub-catchment level. The results of modeling and analyses are presented in Section 4. Finally, key study findings and conclusions are presented in Section 5.

2. Hydrological Modeling

2.1. Study Area

The study area of main stem Tarim River starts from Alar and ends at Taitema Lake (Figure 1). The area is characterized by an extremely arid desert climate with low precipitation and high evapotranspiration. The average annual temperature ranges from 10.6 to 11.5 °C and precipitation from 17.4 to 42.0 mm [19]. In this arid region, the annual reference evapotranspiration may reach 3000 mm and is relatively high in July and August. Because of the region's aridity, no overland flow is generated from rainfall at the alluvial plains of the main stem. Peak flows, caused by melting glacier water in the upper mountain areas of the Tarim River basin, occur in July, August and September. River discharge data is collected from four gauging stations: Alar, Xinqiman, Yingbaza and Qiala (Figure 1).

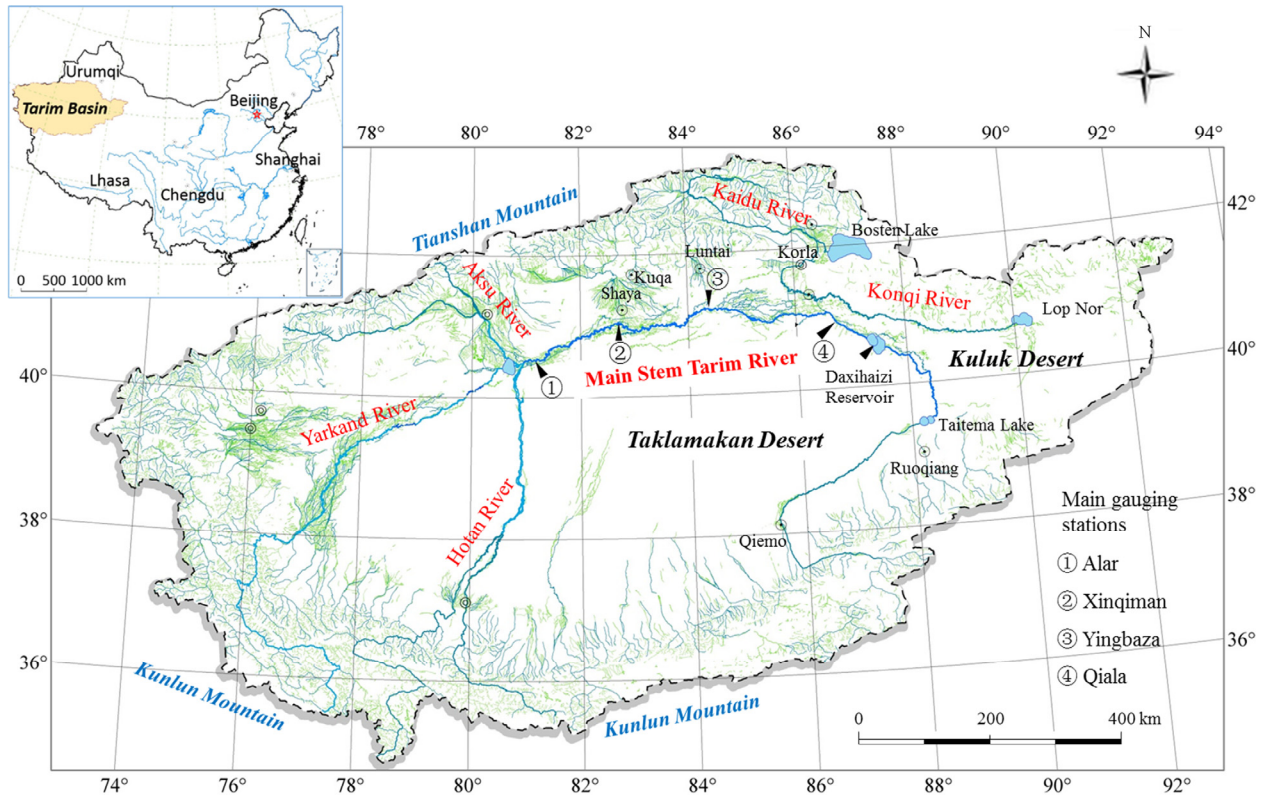


Figure 1. Tarim River basin and main stem river gauging stations.

Average annual discharge in the main stem during the last 60 years is approximately $4.5 \times 10^9 \text{ m}^3$ (Figure 2). Discharge of upper and lower reaches were measured in Alar and Qiala gauging station, respectively. Discharge of the lower reach indicates a significant drop from the 1970s, due to overexploitation of water resources in the upper and middle reaches of the river basin. However, since the Tarim River basin comprehensive management project funded by the Chinese central government was initiated, this decline has reversed during the past decade. The increasing availability of water has had a positive effect on the recovery of the Green Corridor in the lower reach [20]. However, water scarcity still remains a critical problem in this arid region.

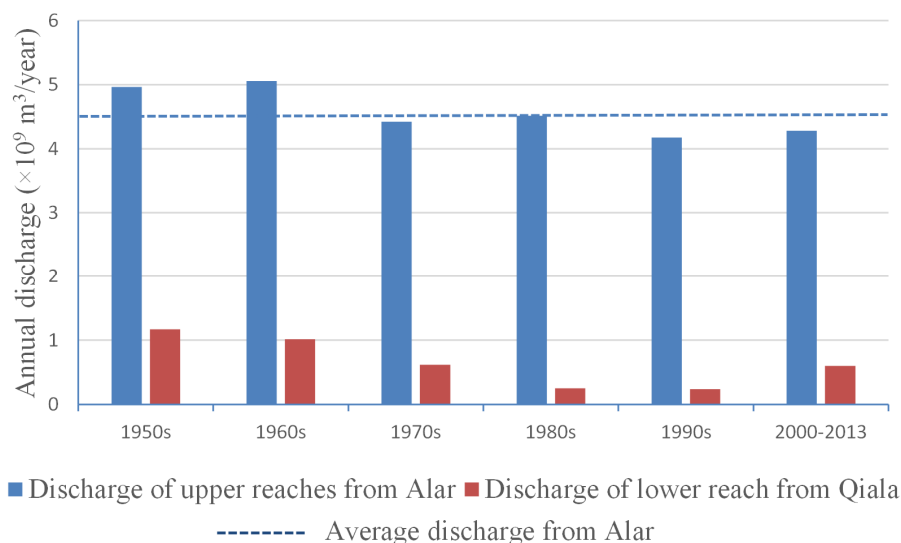


Figure 2. Annual discharge of the main stem Tarim River in the past six decades.

2.2. MIKE HYDRO Model Setup

MIKE HYDRO is a comprehensive deterministic, semi-distributed and physically-based modeling system for the simulation of water flow, water consumption, water quality, and sediment transport. It has an integrated modular structure with basic computational modules for hydrology and hydrodynamics. One basic MIKE HYDRO module is MIKE HYDRO basin, containing modules for evapotranspiration, snow melt, overland and channel flow, crop irrigation, and exchange between aquifer and rivers. A map layer coordinates the parallel running of the process components. Rivers and catchments are depicted in the map layer. Parameters and data requirements are outlined in a tabular layer. Simulation results are obtained from a result layer.

2.2.1. Sub-Catchments and Data

In this study, the study area was divided into four sub-regions, namely Alar-Xinqiman (A), Xinqiman-Yingbaza (B), Yingbaza-Qiala (C), and Qiala-Taitema Lake (D). The sub-regions were named “sub-catchments” in the model (Figure 3) and their borders were automatic delineation from MIKE HYDRO, rather than real catchment borders. Because the hydrological parameters within each sub-catchment were aggregated, the region borders did not affect the simulation. The sub-catchments were separated by the gauging stations shown in Figure 1. In each sub-catchment, the hydrologic parameters were aggregated in an effort to simplify the overall analysis. In the main stem Tarim River, the upper, middle and lower reaches extend from Alar to Yingbaza, Yingbaza to Qiala and Qiala to Taitema Lake, respectively. The borders of sub-catchments are automatic catchment borders from MIKE HYDRO. Because the features in each sub-catchment are lumped together, the shapes of sub-catchment borders does not effect on the simulation results.

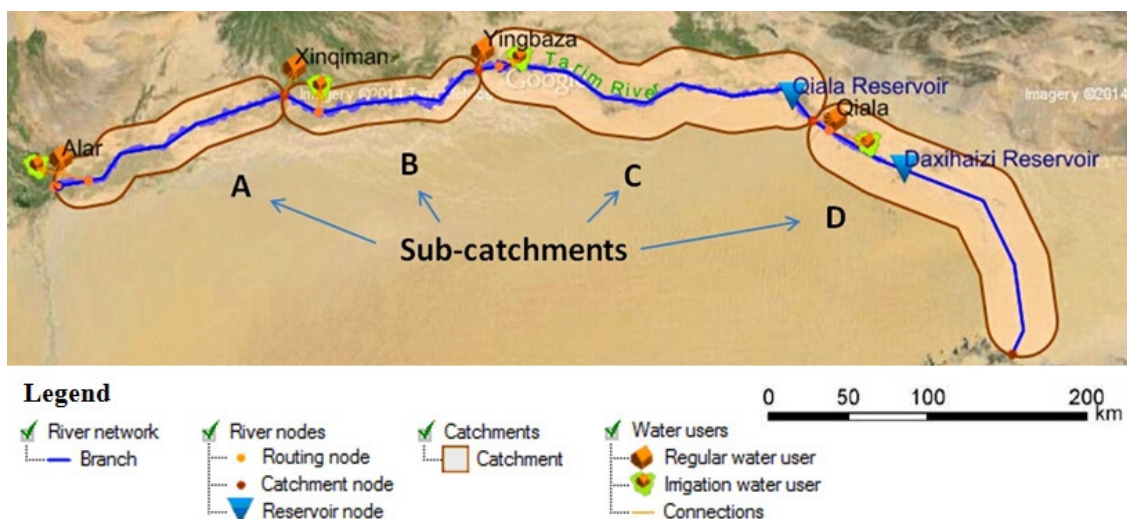


Figure 3. Sub-catchments in the main stem of Tarim River in MIKE HYDRO.

River nodes, branches, catchments, reservoirs, water users and their connections were all specified in a network model (Figure 3). The model design comprised two types of water users considered by MIKE HYDRO: “irrigation water users” (e.g., cotton, wheat and tomatoes) and “regular water users” (non-irrigation water users). Each irrigation water user was assigned with one irrigation field wherein

different irrigation methods, crop modules and soil types were specified. On each irrigated field, a crop sequence was characterized by a crop type, sowing date and reference to the irrigation method used to irrigate the crop. A crop sequence lasted until the end of the previous growth stage [18]. For each regular water user, a water demand time series was specified to represent the total amount of water required to fulfill domestic and ecological water demand in each sub-catchment. In the middle and lower reaches, the Qiala and Daxihaizi reservoirs were included to simulate the operations using operating rule curves. Since both reservoirs had significant surface areas, evaporation and infiltration of reservoirs were factors important to water balance calculations. Data for parameterization in the study were acquired and sorted by Xinjiang Institute of Ecology and Geography, Chinese Academy of Sciences (CAS).

2.2.2. Muskingum Routing

The Muskingum method is a commonly used hydrologic routing method in situations requiring a variable storage-discharge relationship [21]. The Muskingum method models the storage volume of flooding in a river channel. The key parameters in Muskingum routing are travel time (K) and weighting coefficient (X). The value of X depends on the shape of the wedge storage, and ranges from 0 for reservoir-type storage to 0.5 for a full wedge.

The Muskingum method assumes that water surface in the reach is a uniform continuous surface profile between upstream and downstream ends of the section. It also assumes that K and X are constant through the range of flows [22]. The Muskingum parameters K and X are best derived from stream flow measurements. In natural rivers, X has a value between 0 and 0.3 with a mean value of 0.2. Greater accuracy in determining X may not be necessary because the results are relatively insensitive to the value of this parameter. In this MIKE HYDRO model of the Tarim River, X was chosen to be 0.2. The measured K values are shown in Table 1.

Table 1. Muskingum routing parameter K for sub-catchments.

Muskingum Routing	Upper Reaches		Middle Reach	Lower Reach
Sub-Catchment	A	B	C	D
River Length (km)	189	258	398	428
K (h)	51	86	158	198

2.2.3. Crop Factors and Growth Stages

The FAO-56 Dual Crop Coefficient method applied in the model concerns the parameters to be assigned to each crop. Those parameters included the share of the total irrigated area devoted to crops, number of sowing days for each crop, root depth (RD), maximum height (MH), basal crop coefficient (K_{cb}) and length (days) of the growing stage for each crop. Growing stages were categorized as follows: initial stage (INI), development stage (DEV), mid-season (MID), and late season (LAT). Seven crop modules were established in MIKE HYDRO based on field surveys and statistical data (Table 2).

Table 2. Crop factors and growth stages in study area. Data on the share (%) and sowing day were collected from the CAS. Length (days), RD (mm), MH (m), and K_{cb} values were based on a FAO publication [23], with some adjustment based on field surveys of the study area.

Crops	Share (%)	Sowing Day	Length (Days)				RD (mm)	MH (m)	INI	K_{cb}		LAT
			INI	DEV	MID	LAT				MID		
Wheat	2.7	03.21	15	25	40	20	1500	1	0.4	1.2	0.5	
Maize	1.6	04.16	20	25	60	15	1700	2	0.4	1.2	0.7	
Sugarbeet	5.1	03.26	25	35	60	45	1200	0.5	0.5	1.2	0.8	
Bean	1.7	04.21	20	30	30	10	700	0.4	0.4	1.1	0.9	
Melon	2.1	04.01	25	35	40	20	1500	0.4	0.5	1	0.8	
Cotton	82.6	04.21	25	45	50	40	1700	1.5	0.5	1.2	0.8	
Tomato	2.1	04.11	35	40	50	25	1500	0.6	0.5	1.2	0.8	

Parameterization was based on the average values of the irrigated fields in the sub-catchments. K_{cb} was defined as the ratio of crop evapotranspiration over the reference evapotranspiration. In the initial MID and LAT stage, K_{cb} was assumed to be constant and follow a linear variation between INI and MID. The relationship of reference evapotranspiration (ET_0), crop evapotranspiration (ET_c) and actual evapotranspiration (ET_a) is given in Equations (1) and (2) as follows.

$$ET_c = K_{cb} \times ET_0 \quad (1)$$

$$ET_a = K_s \times ET_c \quad (2)$$

where K_s is the water stress coefficient that describes the effect of water stress on crop transpiration and was determined in MIKE HYDRO by considering soil water availability in the irrigated field. Due to the higher performance of the FAO-56 Penman-Monteith method, ET_0 was computed from meteorological data. ET_c was calculated by the crop module, which was influenced by the determination of crop factors [23]. ET_a was calculated by MIKE HYDRO, which identified the actual rate of crop evapotranspiration under the effects of soil water stress.

The sowing days for the crops differs each year due to weather conditions in the study area. Wheat refers to spring wheat in the crop module. Watermelon and muskmelon were considered in the same category as melons. Cotton is the dominant crop in the sub-catchments, representing 82.6% of the total irrigated area. Maximum RDs of cotton depend largely on soil temperature and moisture condition. Soil salinity affects crop development, crop transpiration and, hence, biomass production and harvestable yield. Water in the root zone becomes less available for root extraction when salts build up in the soil profile [24]. In some cases, the cotton root of cotton may reach a depth of 2.2 m to obtain water. After a few tests in the MIKE HYDRO model, the simulation results were not sensitive to the variance of RD around the average level. Therefore, it was regarded as a reliable method for determining average values in the module. Chinese jujube is also widely cultivated in the study area. However, it does not fit into a standard crop module. Therefore, in the model, jujube was considered to be a regular water user rather than an irrigation water user.

2.3. Discharge and Calibration

The MIKE HYDRO model for the main stem Tarim River was calibrated manually for stream flow using monthly data from 2006 to 2008 (Figure 4). The aim of the calibration was to input discharge data to investigate water allocation scenarios, rather than input climate data to investigate river discharge. Therefore, rainfall-runoff model was not essential in the calibration scheme and there were no future predictions. Calibration was mainly conducted on water losses. Evaporation, seepage losses and soil porosity are optimized values in the model calibration. All these three parameters did not possess very large influence on the stream flow. Evaporation data was computed from meteorological data by FAO-56 Penman-Monteith method. Since the climate data was only acquired from Alar meteorological station, the evaporation data along the main stem Tarim River was given a range of 95%–105% for calibration. The calibrated values of evaporation varied slightly different from year to year, and from sub-catchment to sub-catchment. Based on the information collected from the study area, seepage losses were within a range from 0.0007 to 0.0011 by the fraction of seepage losses from stream flow. The calibration results were 0.0007 for all the sub-catchments. Soil porosity was another modified parameter during the calibration. Different types of soil (sand, loam, clay, *etc.*) possessed different ranges of porosities, and the calibrated values varied slightly in different sub-catchments.

NAM automatic calibration was also conducted in the model (Table 3), but it possessed almost no effect on the stream flow. This phenomenon corroborated the theory that because of the region's aridity, no overland flow was generated from rainfall in the study area.

Table 3. Important parameters for NAM automatic calibration.

NAM Parameters	Parameter Descriptions	Units	Value Ranges	Calibrated Values
Umax	Maximum water content in surface storage	mm	10–20	17.79
Lmax	Maximum water content in root zone storage	mm	100–300	166.25
CQOF	Overland flow runoff coefficient	-	0.1–1	0.51
CKIF	Time constant for routing interflow	h	200–1000	533.28
CK1	Time constant 1 for routing overland flow	h	10–50	22.98
CK2	Time constant 2 for routing overland flow	h	10–50	10
TOF	Root zone threshold value for overland flow	-	0–0.99	0.56
TIF	Root zone threshold value for interflow	-	0–0.99	0.53
TG	Root zone threshold value for groundwater recharge	-	0–0.99	0.03
CKBF	Time constant for routing base flow	h	1000–4000	2179.01
CQLOW	Lower base flow, recharge to lower reservoir	percentage	0–100	0
CKLOW	Time constant for routing lower base flow	h	1000–30,000	10,000

The simulation period was not enough to cover the extreme climate situations. Because river discharges of the main stem were around the annual average level in 2006–2008, the simulation results did not take into account the extreme arid years (e.g., in 2009, discharge in the main stem was less than half of the annual average discharge). Since the simulation results were not mainly dependent on climate conditions, as long as it was not an extremely dry year, the study would be suitable for applications in other cases.

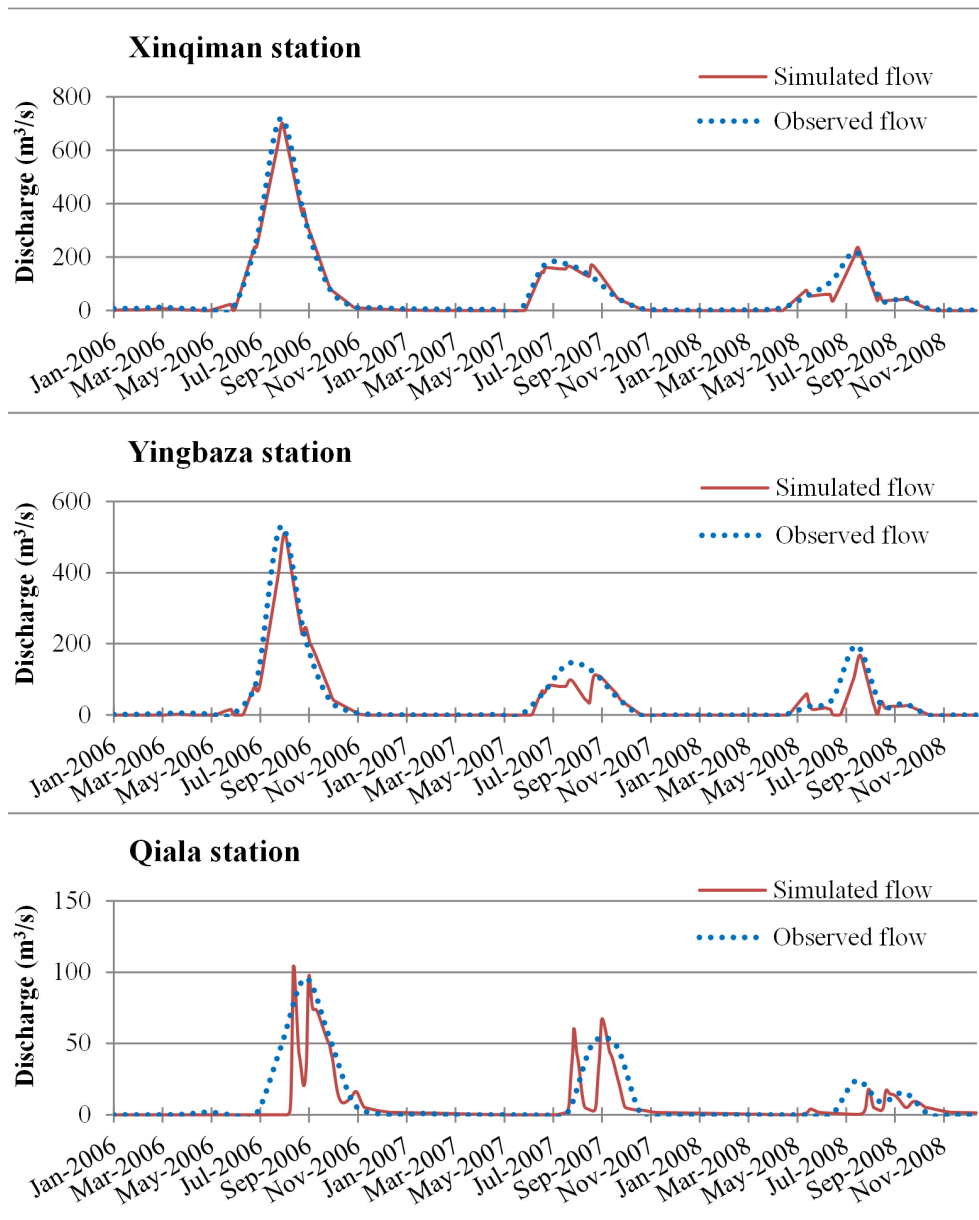


Figure 4. Observed and simulated discharge from three gauging stations: 2006–2008.

The model adequately reproduced the patterns of observed discharges and their magnitudes, although the simulated flow was underestimated. The reason of this underestimation likely resulted from the absence of groundwater in the model. Groundwater is pumped for irrigation in the study area. Since the 1980s, the water table has annually declined at a rate of 20 cm, attributable to increases in water resources development and utilization [9]. In the model, groundwater use was not considered and irrigation was supplied entirely by the surface water. Consequently, the curve for simulated flows would experience an obvious reduction during the crop-growing season compared with that for the observed flow. The simulated peak flow at the Qiala station was lower than the observed flow. Presumably, it was caused by the pumping water from Boston Lake, which increases flows in the lower reach. The influence of this water transfer was evaluated by Xu *et al.* [20], who concluded that the conveyance of water to the lower reach of the Tarim River has a positive effect on local agricultural development and the river ecosystem.

To quantitatively evaluate the performance of the model calibration, four error indices were considered: (a) the Nash-Sutcliffe efficiency (NSE); (b) the root mean square error (RMSE); (c) the RMSE-observations standard deviation ratio (RSR); and (d) the % Bias. NSE is defined in Equation (3) and compares the relative magnitude of squared residuals to the variance of the observed flow [25]. RMSE in Equation (4) is used to examine the square root of the mean squared difference between the observed and simulated flows. RSR standardizes RMSE using the standard deviation in the observations [26] in Equation (5). The % Bias is given in Equation (6) to assess the values of residuals to the observed flow from the gauging stations.

$$NSE = 1 - \frac{\sum_{t=1}^{t=n} [(Q_{sim})_t - (Q_{obs})_t]^2}{\sum_{t=1}^{t=n} [(Q_{obs})_t - (\overline{Q_{obs}})_t]^2} \quad (3)$$

$$RMSE = \sqrt{\frac{1}{n} \sum_{t=1}^{t=n} [(Q_{sim})_t - (Q_{obs})_t]^2} \quad (4)$$

$$RSR = \frac{RMSE}{\sqrt{\frac{1}{n} \sum_{t=1}^{t=n} [(Q_{obs})_t - (\overline{Q_{obs}})_t]^2}} \quad (5)$$

$$\% \text{ Bias} = \frac{\sum_{t=1}^{t=n} [(Q_{sim})_t - (Q_{obs})_t]}{\sum_{t=1}^{t=n} (Q_{obs})_t} \times 100 \quad (6)$$

where Q_{sim} is the simulated discharge (m^3/s), Q_{obs} is the observed discharge (m^3/s), $\overline{Q_{obs}}$ is the mean observed discharge (m^3/s) and n is the number of observations, with time intervals t .

The statistical performances from Table 4 could be considered satisfactory compared to the model evaluation guidelines by Moriasi *et al.* [27]. The simulated discharges were very similar to the observed discharges from the gauging stations, especially the Xinqiman and Yingbaza stations in the upper and middle reaches. Because the efficiency coefficient was sensitive to extreme values, the high values of the NSE (0.88, 0.86 and 0.92) indicated a good match of simulated and observed discharges during flood seasons. RMSE values at the Xinqiman and Yingbaza stations were acceptable in light of the high discharges at both stations. RSR standardizes RMSE by including the standard deviation of the observations, and both values represented good ratings. The increasing tendency of the % Bias from upstream to downstream could be attributed to the absence of groundwater discharge and the pumping of water near the Qiala station. If daily values rather than monthly values are used, it is likely that the calibration would have a lower performance. However, daily time series for the calibration of river flows are not available.

Table 4. Evaluation of calibration performance for three gauging stations: 2006–2008.

Gauging Stations	NSE	RMSE (m^3/s)	RSR	% Bias
Xinqiman	0.88	14.7	0.11	−2.41
Yingbaza	0.86	11.53	0.12	−3.42
Qiala	0.92	3.58	0.10	−8.24

The model was lacking of validation mainly because of data limitation. This problem would have influence on the accuracy of the model, especially on the river discharge, evaporation and seepage losses.

Consequently, the model could not provide reliable quantitative time series data on water losses, but as long as the qualitative effects and the mutual influences of the four sub-catchments were still valid, simulation results on the water consumption and allocation would be reliable. Furthermore, since river discharge data in the model was not generated from rainfall-runoff model, and no future predictions were made by the MIKE HYDRO model, the accuracy of the simulation results would not be largely affected by the absence of validation. Other authors have also experienced similar difficulties when monitoring data were limited [28,29].

3. Design of Scenarios

Based on recent trends in agricultural practices, different scenarios were developed. The proposed scenarios were designed to provide stakeholders and decision makers with improved insight into water scarcity and solutions for agricultural water allocation.

3.1. Irrigation Scenarios

3.1.1. Total Available Water (TAW) Scenarios

When calculating the soil-water balance, the amount of water stored in the root zone can be expressed as an equivalent water depth (W_r) or as root zone depletion (D_r). TAW is the amount of water that a crop can extract from its root zone. Its magnitude depends on the soil type and rooting depth. The water content above field capacity cannot be held against the forces of gravity and will drain out because the water content below the wilting point cannot be extracted by plant roots. Accordingly, TAW in the root zone is the difference between the water content at field capacity and the wilting point. At field capacity, D_r is zero and at the permanent wilting point D_r is equal to TAW [23].

The design of the TAW scenarios assumed that irrigation starts when soil moisture content reaches the specified fraction of TAW. From TAW = 0.7 to TAW = 0.1, seven scenarios were investigated to show the yield performance by different crops. As crop yield declined with the decrease of TAW, the primary purpose of the scenarios was to find the suitable fraction of TAW for each crop at which less water is consumed while maintaining a relatively high crop yield.

Irrigation is essential for stabilizing and increasing crop yields. Stewart [30] derived the relationship between the decrease in relative yield and the relative evapotranspiration deficit. The water use-yield relationship was determined using Equation (7).

$$\left(1 - \frac{Y_a}{Y_m}\right) = K_y \left(1 - \frac{ET_a}{ET_c}\right) \quad (7)$$

where Y_a is the actual harvest yield (t/ha), Y_m is the maximum harvest yield (t/ha) and K_y is the yield response factor representing the effect of reduction in evapotranspiration on lost yield. K_y values were obtained from FAO Irrigation and Drainage Paper No. 33 [31].

3.1.2. Water-Saving Irrigation Scenarios

In the study area, the implementation of water-saving irrigation is developing rapidly by the method of drip irrigation under mulch (DIUM). By applying DIUM method in the irrigation fields, spray loss

(SL) and wetting fraction (WF) will be significantly reduced compared with sprinkler irrigation. SL corresponds to the fraction of irrigation water that is evaporated before reaching the soil surface. WF determines the fraction of field surface being wetted during irrigation. SL and WF values are calculated from Equations (8) and (9):

$$SL = SL_S \times \%SL_S + SL_D \times \%SL_D \quad (8)$$

$$WF = WF_S \times \%WF_S + WF_D \times \%WF_D \quad (9)$$

where SL_S is the SL for sprinkler irrigation, SL_D is the SL for DIUM, WF_S is the WF for sprinkler irrigation, WF_D is the WF for DIUM. Each of these parameters is multiplied by its percentage applied in the irrigated fields. Only the sprinkler irrigation and DIUM methods were considered in this scenario. Consequently, the sum of $\%SL_S$ and $\%SL_D$ as well as the sum of $\%WF_S$ and $\%WF_D$ were assumed to be 1.

DIUM is mainly applied in the cotton fields where the ground surface was approximately 80% covered with transparent polythene film as mulch [32]. SL is set to be 0.5 for sprinkler irrigation and 0.1 for DIUM in the model. WF is close to 1 in sprinkler irrigation and reduced to 0.1 for DIUM in MIKE HYDRO irrigation module [18].

Five water-saving scenarios were designed based on the percentage of DIUM applied in the total irrigated area, 10%, 30%, 50%, 70% and 100%, respectively. The primary goal of these scenarios was to investigate how much water could be saved by applying DIUM to the irrigated fields.

3.2. Land Use Scenarios

Three land-use scenarios were designed based on the information collected from farmers, surveys, interviews with decision makers in the region, and the Tarim River basin water resources management ordinance in Xinjiang Uygur Autonomous Region. The ordinance was created by the local government for the sustainable management of water resources. The impetus for these scenarios included eco-system protection, high prices of agricultural products and government regulations restricting agricultural water use in the Tarim River basin. In each sub-catchment the hydrological features were lumped together, so the spatial distribution of land use within each sub-catchment was not considered. The land use scenarios were considered among the sub-catchments. The three scenarios included the agricultural land use decrease scenario (LUD scenario), the land use increase scenario (LUI scenario) and crop type change scenario (CTC scenario). These scenarios were considered independently based on practical situations and local policies.

The LUD scenario reflects the government policy to restrict agricultural water use in the upstream, thus increasing free-flowing water for downstream areas. Under this scenario, approximately 20% of the agricultural land would be abandoned in sub-catchments A and B.

The LUI scenario assumes more available water in downstream areas resulting from new water conveyance projects in the lower reach [20]. Under this scenario, the amount of new agricultural farmland in sub-catchment D would be increased by 20%.

The CTC scenario reflects the proposal for using less irrigation water by substituting different types of crops. Apocynum grows in the arid climate of Central Asia and provides an income for local people. It withstands higher levels of soil salinity and consumes less water than cotton [33]. Apocynum is used

as a medicinal plant and a fiber crop. The leaves provide raw material for tea and the stems provide raw material for the textile and paper industries. The CTC scenario assumed that 20% of the cotton would be replaced by apocynum in all the sub-catchments.

4. Results and Discussion

4.1. Actual Crop Evapotranspiration (ET_a) and Deep Percolation (DP)

While ET_a refers to the upward loss of water by the vegetated surface, deep percolation (DP) is defined as the downward movement of water through the soil profile beyond the root zone. The results of simulations for ET_a and DP in the four sub-catchments are shown in Figure 5. ET_a primarily occurs from June to September, while DP primarily appears in a shorter period from July to August. Compared with ET_a , the shorter period of DP may be due to low soil moisture, which restricts crop growth in this arid region [34]. The rapid increase and decrease of DP at the beginning and end period indicates that DP mainly occurs when soil moisture reach a certain content. ET_a conformed to DP in a slowly increasing trend from sub-catchment A to B and from B to C. In sub-catchment D, both factors showed a dramatic drop, reflecting the water shortage in this lower reach [5]. The total ET_a for 2006 in sub-catchments A–D was 666, 709, 864 and 190 mm, respectively. This reflected high water stress in the lower reach of sub-catchment D. The highest levels of ET_a and DP both occurred in sub-catchment C during July. Irrigation water consumption was relatively high in this district. In the non-growing season, there was no ET_a or DP. This finding was consistent with Yuan *et al.* [35], who found that in the early and late stage of the dormancy period of vegetation, ET_a was approximately zero, whereas the level of ET_c was still large.

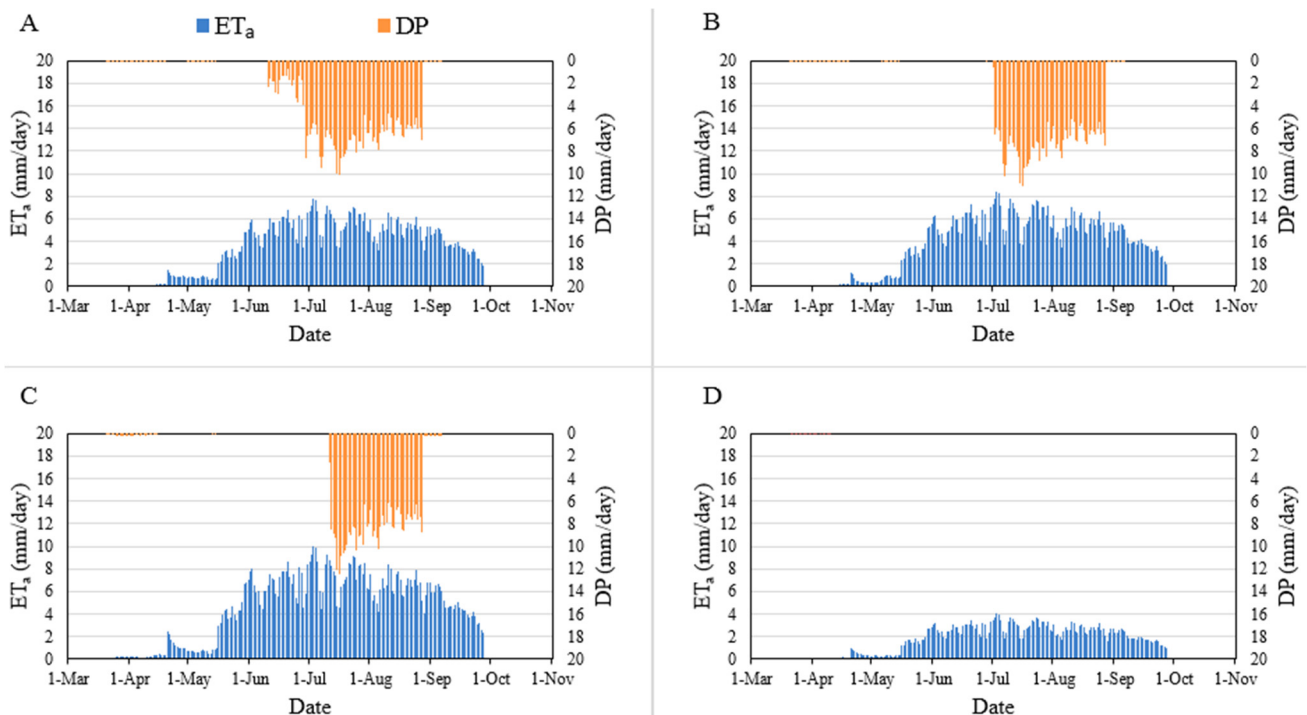


Figure 5. Actual crop evapotranspiration (ET_a) and deep percolation (DP) in sub-catchments A–D during the crop-growing season.

4.2. Effects of Scenarios

4.2.1. Irrigation Scenarios

Total Available Water (TAW) Scenarios

Optimal crop production depends greatly on available soil water [36]. Analyzing crop yields for every crop type under the same conditions of water scarcity represents a sensitivity analysis. It shows the highly differing susceptibility of crop types to water stress.

Figure 6 demonstrates robustness in the performance of cotton yield with reductions in the fraction of TAW. The yield of ginned cotton dropped 6%, from TAW of 0.7 to TAW of 0.4. The yields of wheat and bean also showed robust performances when irrigation water was decreased. Crop yields in response to TAW were investigated beginning at 0.7, where none of the crops suffered a reduction in yield. At a TAW of 0.6, most crops maintained a relatively high yield without a rapid decrease, except for tomatoes. Nearly half of the tomato production was stopped due to lack of water at TAW of 0.4. This demonstrated that tomatoes should be considered only in areas where the supply of irrigation water is ensured. At the same level of TAW, the yield of maize, sugarbeet and melon suffered a significant decline. However, because cotton was the most important crop in the Tarim River basin [37], its cultivation should be prioritized in areas where optimum conditions can be maintained. To maintain cotton production at relatively high levels, irrigation at a TAW level of 0.4 is recommended.

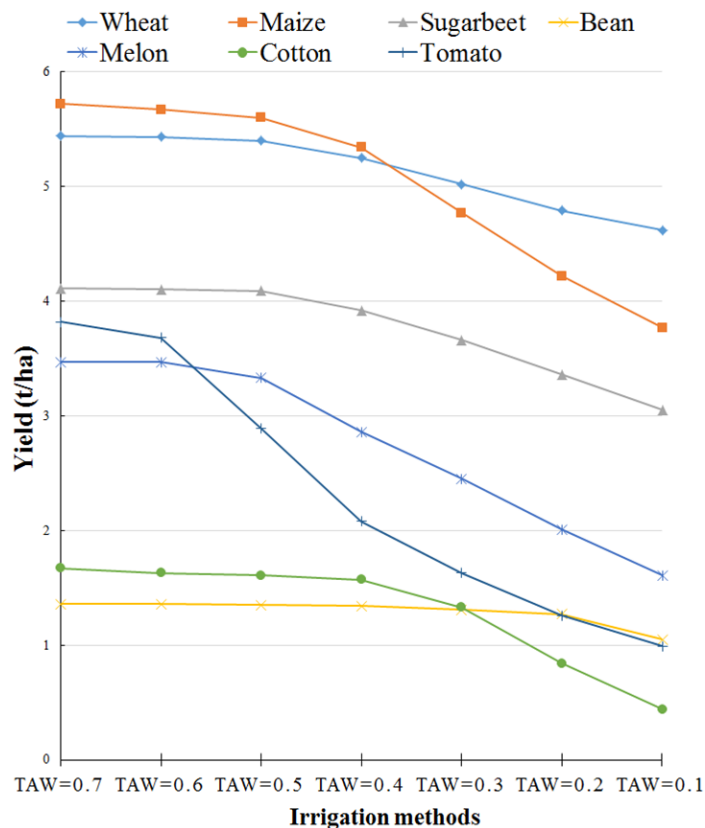


Figure 6. Irrigation scenarios based on fraction of total available water (TAW). Average yield performance of crops showing in the whole irrigation field within three-year simulation period.

Water-Saving Irrigation Scenarios

Spray loss (SL) and wetting fraction (WF) showed marked reductions with an increase in the percentage of DIUM applied in irrigated fields (Table 5), whereas water saving (WS) and reduction of water demand deficit (RWDD) showed positive effects. WS was only 6% and RWDD was only 5% when DIUM represented 10% of total irrigation. However, WS and RWDD increased to 40% and 30%, respectively, when the level of DIUM applied to all irrigated fields was 100%. This indicates the potential value of DIUM for saving water and reducing water deficits. Even when DIUM is at 50%, WS and RWDD reflected notable changes at 25% and 16%, respectively. When DIUM increased from 10% to 100%, SL decreased from 46% to 10% and WF reduced from 91% to 10%. This reflects the substantial benefits to water savings resulting from the application of these technologies.

Table 5. Summary of five DIUM scenarios.

% DIUM	% SL	% WF	% WS	% RWDD
10	46	91	6	5
30	38	73	17	12
50	30	55	25	16
70	22	37	32	22
100	10	10	40	30

Results of modeling reveal that a considerable amount of water could be saved in with the introduction of water-saving irrigation. Considering the effort of applying DIUM on the irrigated fields, it was an arduous task to immediately raise the DIUM to 100%. However, even at DIUM of 70%, significant potential for saving water and reducing the water demand deficit exists. RWDD was slightly less affected than WS by the increase of DIUM. However, this abatement could result in a crucial change in water scarcity, with the highest value of 30% on the irrigated fields. Similar results were reported by Hu *et al.* [38], who concluded that water-saving economical irrigation can greatly increase water use efficiency.

4.2.2. Land Use Scenarios

The effects of the scenarios on irrigation water demand and water deficits at the sub-catchment level are shown in Figure 7.

In the LUD scenario, the reduction of farmland in sub-catchments A and B indicates a positive effect on the reduction of irrigation water demand. A substantial decline of 100 mm irrigation water demand could be achieved in the upper reaches. Moreover, LUD possessed a broader potential benefit on % irrigation water deficit reduction. All the sub-catchments showed notable decrease on water deficit. A similar land use investigation on the headwater tributary of Tarim River was conducted by Huang *et al.* [13], who found that the expansion of irrigation area ultimately leads to the increase in water consumption and reduces water availability.

In the LUI scenario, irrigation water demand was raised by nearly 50 mm with the increase of farmland in the lower reach. % irrigation water deficit was also increased by over 25% in the region. Since the increase of farmland in the upper and middle reaches had already been strictly restricted by the local government policies, the increase of farmland in the lower reach was also found to be harmful to the water saving purpose, and therefore should not be recommended.

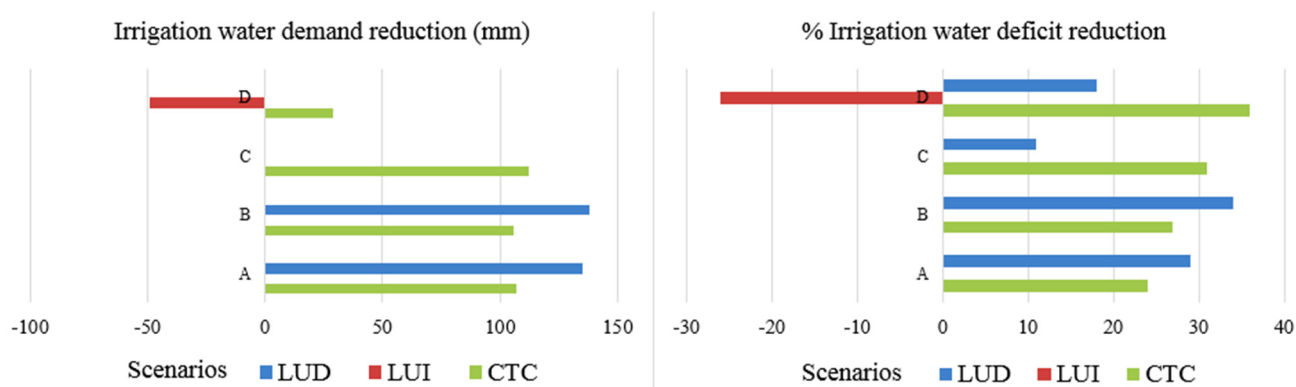


Figure 7. Effects of land use scenarios LUD (land use decrease), LUI (land use increase) and CTC (crop type change), with irrigation water demand reduction and % irrigation water deficit reduction as indicators in sub-catchments A–D.

In the CTC scenario, both irrigation water demand and % irrigation water deficit were largely reduced in all sub-catchments. Irrigation water demand dropped over 100 mm in the upper and middle reaches. % Irrigation water deficits were also significantly decreased, with a maximum reduction of 36% in the lower reach. Rotation of crop types can be an effective approach to reduce irrigation water demand and deficit. Therefore, scenario CTC is recommended for future land use developments.

5. Conclusions

The MIKE HYDRO model adequately represented the river discharge and irrigation water allocation in the main stem Tarim River. By adapting the K_{cb} values, the actual evapotranspiration could also be reliably simulated. In general, the model performed satisfactorily.

In 2006, the total ET_a in sub-catchments A–D was 666, 709, 864 and 190 mm, respectively, which illustrates the condition of high water stress for crops in the lower reach of sub-catchment D. Meanwhile, the highest ET_a and DP both occurred in sub-catchment C. Irrigation water consumption was relatively high in this district.

Optimal crop production depends greatly on available soil water. Cotton demonstrates a robust yield performance with a reduction in the fraction of TAW. The yield of ginned cotton dropped 6%, from TAW of 0.7 to TAW of 0.4. To maintain cotton production at a relatively high level, while reducing total water use, a TAW of 0.4 is recommended. Wheat, maize, sugar beets, beans, melons and cotton all showed a higher compatibility with water stress compared with tomatoes. Tomatoes should be grown only in areas where the supply of irrigation water is ensured.

WS and RWDD increased to 40% and 30%, respectively, with DIUM at 100% in all irrigated fields. This indicates the potential value of DIUM in saving water and reducing water deficits. DIUM could largely ameliorate the water shortage in the lower reach, where the natural Tugai vegetation is functioning as an important ecosystem by restraining dust. This water-saving technique should be applied whenever possible.

A considerable reduction in the demand for irrigation water and water deficits can be achieved by changing land use. Over 100 mm of irrigation water demand was saved by reducing the amount of farmland in sub-catchments A and B. In both sub-catchments, irrigation water deficit decreased by more than 25%. Reduced areas of farmland in the upper reaches could have considerable benefits for all the

sub-catchments. The substitution of apocynum for cotton could be an effective approach in reducing irrigation water demand and water deficit. Therefore, scenario CTC is recommended for future land use developments in the region.

The most important feature of the MIKE HYDRO model is the clarification of the mutual interference of the sub-catchments along the main stem Tarim River. Issues of agricultural water consumption and allocation cannot be effectively managed in separate regions. Clear evidence was presented to provide stakeholders and decision makers with relevant information about the anticipated effects of each scenario. Because the hydrological model has already been established in the study area, future simulations of water availability and allocation can be undertaken. Groundwater and the spatial distribution of water users in the sub-catchments will be addressed in the next phase of our research. The results of MIKE HYDRO simulations can contribute to decision-making for sustainable management of water and land use in the Tarim River basin.

Acknowledgments

This study was supported by German-Sino bilateral collaboration research project SuMaRiO funded by the German Federal Ministry of Education and Research. Within SuMaRiO research group, we are grateful to Thevs Niels and Shamaila Zia-Khan's work, which helped the progress of our research. We thank our partners from the Xinjiang Institute of Ecology and Geography, Chinese Academy of Sciences who helped with our fieldwork and provided the basic data and information in the cooperated project (NSFC-UNEP, No. 41361140361). Suggestions and comments by the two reviewers on this paper are greatly appreciated. This work was supported by the German Research Foundation (DFG) and the Technische Universität München within the Open Access Publishing Funding Programme.

Author Contributions

The manuscript was written by Yang Yu and Philipp Huttner. The MIKE HYDRO model was developed and analyzed by Yang Yu and Markus Disse. Data was collected and sorted by Yang Yu, Ruide Yu, Guoan Yu and Lingxiao Sun. Additional information and outcomes from SuMaRiO German side were collected by Christian Rumbaur. Figures and Tables were provided by Yang Yu, Guoan Yu and Markus Disse.

Conflicts of Interest

The authors declare no conflict of interest.

References

1. Schmitz, C.; Lotze-Campen, H.; Gerten, D.; Dietrich, J.P.; Bodirsky, B.; Biewald, A.; Popp, A. Blue water scarcity and the economic impacts of future agricultural trade and demand. *Water Resour. Res.* **2013**, *49*, 3601–3617.
2. Cai, X.M.; Rosegrant, M.W. Optional water development strategies for the Yellow River Basin: Balancing agricultural and ecological water demands. *Water Resour. Res.* **2004**, *40*, doi:10.1029/2003WR002488.

3. Chen, Y.; Xu, Z. Plausible impact of global climate change on water resources in the Tarim River Basin. *Sci. China Ser. D Earth Sci.* **2005**, *48*, 65–73.
4. Chen, Y.; Zhang, X.; Zhu, X.; Li, W.; Zhang, Y.; Xu, H. Analysis on the ecological benefits of the stream water conveyance to the dried-up river of the lower reaches of Tarim River, China. *Sci. China Ser. D Earth Sci.* **2004**, *47*, 1053–1064.
5. Thevs, N. Water scarcity and allocation in the Tarim Basin: Decision structures and adaptations on the local level. *J. Curr. Chin. Aff.* **2011**, *40*, 113–137.
6. Chen, Y.N.; Takeuchi, K.; Xu, C.; Chen, Y.P.; Xu, Z.X. Regional climate change and its effects on river runoff in the Tarim Basin, China. *Hydrol. Process.* **2006**, *20*, 2207–2216.
7. Hao, X.M.; Chen, Y.; Xu, C.; Li, W. Impacts of climate change and human activities on the surface runoff in the Tarim River Basin over the last fifty years. *Water Resour. Manag.* **2008**, *22*, 1159–1171.
8. Ling, H.B.; Xu, H.L.; Fu, J.Y. High- and low-flow variations in annual runoff and their response to climate change in the headstreams of the Tarim River, Xinjiang, China. *Hydrol. Process.* **2013**, *27*, 975–988.
9. Feng, Q.; Endo, K.N.; Cheng, G.D. Towards sustainable development of the environmentally degraded arid rivers of China—a case study from Tarim River. *Environ. Geol.* **2001**, *41*, 229–238.
10. Qi, F.; Wei, L.; Jianhua, S.; Yonghong, S.; Yewu, Z.; Zongqiang, C.; Haiyang, X. Environmental effects of water resource development and use in the Tarim River basin of northwestern China. *Environ. Geol.* **2005**, *48*, 202–210.
11. Hao, X.; Chen, Y.; Li, W. The driving forces of environmental change during the last 50 years in the Tarim River Basin. *Acta Geogr. Sin.* **2006**, *61*, 262–272.
12. Chen, Y.; Ye, Z.; Shen, Y. Desiccation of the Tarim River, Xinjiang, China, and mitigation strategy. *Quat. Int.* **2011**, *244*, 264–271.
13. Huang, S.; Krysanova, V.; Zhai, J.; Su, B. Impact of intensive irrigation activities on river discharge under agricultural scenarios in the semi-arid Aksu River basin, northwest China. *Water Resour. Manag.* **2015**, *29*, 945–959.
14. Arnold, J.G.; Srinivasan, R.; Muttiah, R.S.; Williams, J.R. Large area hydrologic modeling and assessment part I: Model development. *J. Am. Water Resour. Assoc.* **1998**, *34*, 73–89.
15. Biancamaria, S.; Bates, P.D.; Boone, A.; Mognard, N.M. Large-scale coupled hydrologic and hydraulic modeling of the Ob river in Siberia. *J. Hydrol.* **2009**, *379*, 136–150.
16. Paz, A.R.; Bravo, J.M.; Allasia, D.; Collischonn, W.; Tucci, C.E.M. Large-Scale hydrodynamic modeling of a complex river network and floodplains. *J. Hydrol. Eng.* **2010**, *15*, 152–165.
17. Gunduz, O. Coupled Flow and Contaminant Transport Modeling in Large Watersheds. Ph.D. Thesis, Georgia Institute of Technology, Atlanta, GA, USA, 2004.
18. Danish Hydraulic Institute (DHI). *MIKE HYDRO User Manual*; DHI: Hoersholm, Denmark, 2014.
19. Chen, Y.N.; Xu, C.C.; Hao, X.M.; Li, W.H.; Chen, Y.P.; Zhu, C.G. Fifty-Year climate change and its effect on annual runoff in the Tarim River Basin, China. *Quat. Int.* **2009**, *208*, 53–61.
20. Xu, H.; Ye, M.; Li, J. The water transfer effects on agricultural development in the lower Tarim River, Xinjiang of China. *Agric. Water Manag.* **2008**, *95*, 59–68.
21. Chow, V.T.; Maidment, D.R.; Mays, L.W. *Applied Hydrology*; Tata McGraw-Hill Education: New York, NY, USA, 1988; p. 572.
22. Veissman, W.; Lewis, G.L. *Introduction to Hydrology*, 5th ed.; Prentice Hall: Upper Saddle River, NJ, USA, 2003; p. 612.

23. Allen, R.G.; Pereira, L.S.; Raes, D.; Smith, M. *Crop Evapotranspiration—Guidelines for Computing Crop Water Requirements*; FAO Irrigation and Drainage Paper 56; FAO: Rome, Italy, 1998; Volume 300.
24. Steduto, P.; Hsiao, T.C.; Fereres, E.; Raes, D. *Crop Yield Response to Water*; FAO: Rome, Italy, 2012; pp. 17–40.
25. Nash, J.; Sutcliffe, V. River flow forecasting through conceptual models, part I—A discussion of principles. *J. Hydrol.* **1970**, *10*, 282–290.
26. Legates, D.R.; McCabe, G.J. Evaluating the use of “goodness-of-fit” measures in hydrologic and hydroclimatic model validation. *Water Resour. Res.* **1999**, *35*, 233–241.
27. Moriasi, D.N.; Arnold, J.G.; van Liew, M.W.; Bingner, R.L.; Harmel, R.D.; Veith, T.L. Model evaluation guidelines for systematic quantification of accuracy in watershed simulations. *Trans. ASABE* **2007**, *50*, 885–900.
28. Girolamo, D.; Porto, L. Land use scenario development as a tool for watershed management within the Rio Mannu Basin. *Land Use Policy* **2012**, *29*, 691–701.
29. Molina-Navarro, E.; Trolle, D.; Martínez-Pérez, S.; Sastre-Merlín, A.; Jeppesen, E. Hydrological and water quality impact assessment of a Mediterranean limno-reservoir under climate change and land use management scenarios. *J. Hydrol.* **2014**, *509*, 354–366.
30. Stewart, J.I.; Hagan, R.M.; Pruitt, W.O.; Danielson, R.E.; Franklin, W.T.; Hanks, R.J.; Riley, J.P.; Jackson, E.B. *Optimizing Crop Production through Control of Water and Salinity Levels in the Soil*; Utah State University: Logan, UT, USA, 1977; p. 67.
31. Doorenbos, J.; Kassam, A.H. *Yield Response to Water*; Irrigation and Drainage Paper; FAO: Rome, Italy, 1979; Volume 33, p. 257.
32. Zia-Khan, S.; Spreer, W.; Pengnian, Y.; Zhao, X.; Othmanli, H.; He, X.; Müller, J. Effect of dust deposition on stomatal conductance and leaf temperature of cotton in northwest China. *Water* **2014**, *7*, 116–131.
33. Thevs, N.; Zerbe, S.; Kyosev, Y.; Rozi, A.; Tang, B.; Abdusalih, N.; Novitskiy, Z. *Apocynum venetum* L. and *Apocynum pictum* Schrenk (Apocynaceae) as multi-functional and multi-service plant species in Central Asia: A review on biology, ecology, and utilization. *J. Appl. Bot. Food Qual.* **2012**, *85*, 159–167.
34. Ma, X.; Chen, Y.; Zhu, C.; Li, W. The variation in soil moisture and the appropriate groundwater table for desert riparian forest along the Lower Tarim River. *J. Geogr. Sci.* **2011**, *21*, 150–162.
35. Yuan, G.; Zhang, P.; Shao, M.A.; Luo, Y.; Zhu, X. Energy and water exchanges over a riparian *Tamarix* spp. stand in the lower Tarim River basin under a hyper-arid climate. *Agric. For. Meteorol.* **2014**, *194*, 144–154.
36. Stričević, R.; Čaki, E. Relationships between available soil water and indicators of plant water status of sweet sorghum to be applied in irrigation scheduling. *Irrig. Sci.* **1997**, *18*, 17–21.
37. Liu, Y.; Chen, Y. Impact of population growth and land-use change on water resources and ecosystems of the arid Tarim River basin in western China. *Int. J. Sustain. Dev. World Ecol.* **2006**, *13*, 295–305.
38. Hu, S.; Song, Y.; Zhou, H.; Tian, C. Experimental study on water use efficiency of cotton in the Tarim River Basin. *Agric. Res. Arid Areas* **2001**, *20*, 66–70.